Heliyon 6 (2020) e04282

Contents lists available at ScienceDirect

Heliyon

journal homepage: www.cell.com/heliyon

Research article

Bio-inspired wideband antenna for wireless applications based on perturbation technique

Jeremiah O. Abolade [a,*], Dominic B.O. Konditi [b], Vasant M. Dharmadhikary [c]

[a] Department of Electrical Engineering, Pan African University, Institute for Basic Sciences, Technology and Innovation, Jomo Kenyatta University of Agriculture and Technology, Juja, Kenya
[b] School of Electronic and Communication Engineering, The Technical University of Kenya, Nairobi, Kenya
[c] Department of Electrical and Electronic Engineering, Dedan Kimathi University of Technology, Nyeri, Kenya

ARTICLE INFO

Keywords:
Electrical engineering
Computer engineering
Electrical system
Wireless network
Communication system
Electromagnetics
Bio-inspired
Wideband antennas
Perturbation
Finite element method (FEM)
Carica Papaya-leaf
Fifth-generation (5G)

ABSTRACT

The evolution of advancement in communication technologies and ever-increasing demand by users for compact communication devices has necessitated a shift in the design approach to achieve antenna structures that are compact and robust. Owing to the diverse communication requirements, antenna systems operating across wide bands have become a necessity. An antenna that is capable of working effectively in several bands is called wideband antenna. In this work, a bio-inspired microstrip antenna (Bi-MPA) for wideband application is proposed and simulated. The radiating patch of the proposed Bi-MPA is the shape of *Carica Papaya* leaf. The structure was realized through the perturbation of the circular shape patch. The proposed antenna has an impedance bandwidth of 4.3 GHz (1.9 GHz–6.2 GHz) at a return loss of 10 dB while it exhibits a narrow band at 7.2 GHz (6.99–7.44 GHz) and 9.3 GHz (9.15–9.35 GHz) bands. The gain of the proposed antenna is between 2.60 dB and 10.22 dB and the radiation pattern is quasi-omnidirectional. The proposed Bi-MPA is compact and suitable for global system for mobile communication (GSM1900), Universal Mobile Telecommunication System (UMTS), Wireless Local Area Network (WLAN), Long Term Evolution (LTE2300 and LTE2600), Worldwide Interoperability for Microwave Access (WiMAX), C-band, X-band, and sub6 GHz fifth-generation (5G) band. Our contribution to the scientific community in this work is that we have proposed a single antenna structure that is suitable for communication in all the bands mentioned in order to ensure compactness in the mobile devices as compared to base station antennas.

1. Introduction

The advancement in technology and the evolution of communication standards has led to the need for low-profile antenna structures that can be easily integrated. Microstrip antenna fits well into this requirement, but comes with its challenges such as narrow bandwidth, low gain, and poor radiation efficiency. Over the years, several researches have been directed towards optimizing one or two of these challenges. Moreover, the evolution of communication standards has necessitated the need for wideband, multiband, or Ultrawideband (UWB). For example, some of the commonly used bands in mobile communications are GSM bands (890–960 GHz; 1.71–1.99 GHz), UMTS (1.90–2.2 GHz; 2.5–2.7 GHz), WLAN (2.4–2.484 GHz, 5.15–5.35 GHz, and 5.725–5.825 GHz), WiMAX (3.3–3.69 GHz and 5.25–5.85 GHz) sub6 GHz band proposed for 5G (3.4–3.6 GHz for Russia and 4.4–4.99 GHz for china). It has been shown that all these standards have to work together. Hence, there is a need for a single antenna element suitable for all this band in order to ensure compactness in the mobile devices as compared to base station antennas. The studies in [1, 2, 3, 4, 5, 6, 7, 8, 9] and [10] are some of the recently developed wideband MPA.

The Authors in [1] proposed a stair structure dielectric antenna with an open-ended slot on the ground plane of dimensions 25 × 27 mm^2 for the optimization of the impedance bandwidth and the axial ratio for wideband application. The proposed antenna has a fractional bandwidth of 71.7% (3.844–8.146 GHz) at a return loss (RL) of 10 dB, a 3.9 dBic maximum gain, and 90% radiation efficiency (RE). Similarly, authors in [2] proposed a slot-loaded antenna patch of dimension 0.7λo × 0.47λo × 0.084 λo for wideband operating from 1.62 GHz to 2.78 GHz (52.7% fractional bandwidth) with the aid of L-slot on the ground plane, dual vertical wall and vias. Authors in [3] used a linear array to achieve a

* Corresponding author.
E-mail address: aboladejeremiah@yahoo.com (J.O. Abolade).

https://doi.org/10.1016/j.heliyon.2020.e04282
Received 14 May 2020; Received in revised form 10 June 2020; Accepted 19 June 2020

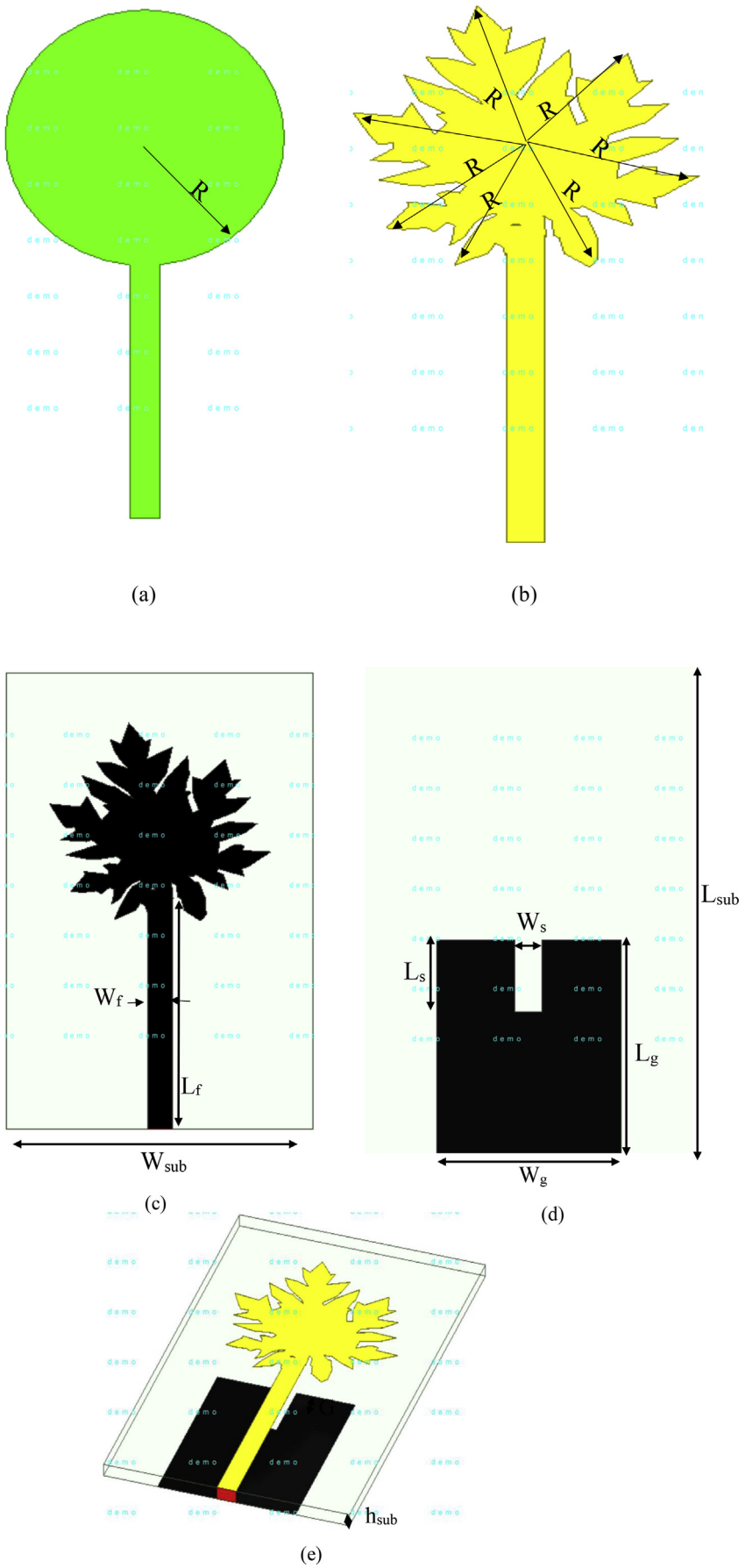

Figure 1. Proposed antenna design (a) initiator circular patch (b) composite Bi-MPA (c) Front view (d) Bottom view and (e) 3D view of the proposed Bi-MPA.

Table 1. Proposed Bi-MPA design parameters.

S/N	Parameter	Description	Value (mm)
1	R	Radius of the circular patch initiator	13.00
2	W_f	Width of the feedline	2.80
3	L_f	Length of the feedline	30.00
4	W_{sub}	Width of the substrate	35.70
5	L_{sub}	Length of the substrate	59.25
6	W_g	Width of the ground plane	20.00
7	L_g	Length of the ground plane	26.00
8	W_s	Width of the rectangular strip	3.00
9	L_s	Length of the rectangular strip	8.75
10	h_{sub}	Height of the substrate	1.58
11	G	Ground-patch gap	2.00

Table 2. The design data (x-y-z coordinates) of each point of the proposed Bi-MPA.

Point	Coordinate (mm)			Point	Coordinate (mm)			Point	Coordinate (mm)			Point	Coordinate (mm)			Point	Coordinate (mm)		
	x	y	z		x	y	z		x	y	z		x	y	z		x	y	z
A	0.0	11.5	0.0	A_1	-12.8	-3.6	0.0	A_2	-3.5	7.6	0.0	A_3	7.0	3.4	0.0	A_4	8.4	-3.2	0.0
B	2.3	12.8	0.0	B_1	-10.4	-1.7	0.0	B_2	-3.0	7.7	0.0	B_3	7.8	4.0	0.0	B_4	7.9	-2.3	0.0
C	1.9	9.3	0.0	C_1	-10.7	-1.1	0.0	C_2	-3.2	1.1	0.0	C_3	7.9	4.5	0.0	C_4	7.6	-2.2	0.0
D	3.3	8.5	0.0	D_1	-8.2	-1.5	0.0	D_2	-1.4	8.9	0.0	D_3	9.9	5.3	0.0	D_4	7.6	-2.4	0.0
E	1.6	7.6	0.0	E_1	-9.7	1.4	0.0	E_2	-0.2	6.2	0.0	E_3	12.1	5.4	0.0	E_4	8.0	-3.2	0.0
F	0.2	6.8	0.0	F_1	-6.3	0.8	0.0	F_2	0.8	5.9	0.0	F_3	12.8	4.7	0.0	F_4	8.6	-3.9	0.0
G	1.4	5.9	0.0	G_1	-4.1	-0.8	0.0	G_2	0.0	7.9	0.0	G_3	11.5	2.8	0.0	G_4	9.9	-4.6	0.0
H	2.1	6.6	0.0	H_1	-3.6	-0.4	0.0	H_2	0.2	11.3	0.0	H_3	10.0	2.5	0.0	H_4	10.7	-5.7	0.0
I	2.3	6.0	0.0	I_1	-5.6	0.7	0.0	I_2	1.4	9.8	0.0	I_3	9.7	2.1	0.0	I_4	10.1	-5.5	0.0
J	3.5	7.9	0.0	J_1	7.0	1.9	0.0	J_2	2.6	6.9	0.0	J_3	8.2	1.9	0.0	J_4	8.8	-5.3	0.0
K	6.0	9.1	0.0	K_1	-8.6	3.2	0.0	K_2	4.1	6.8	0.0	K_3	7.8	1.3	0.0	K_4	8.5	-5.9	0.0
L	4.7	5.9	0.0	L_1	-6.1	3.4	0.0	L_2	2.6	8.7	0.0	L_3	9.9	1.5	0.0	L_4	9.3	-6.8	0.0
M	-4.6	-5.2	0.0	M_1	-5.3	3.1	0.0	M_2	3.0	9.8	0.0	M_3	9.5	2.0	0.0	M_4	8.9	-7.4	0.0
N	-4.0	-4.5	0.0	N_1	-3.9	2.9	0.0	N_2	3.7	9.6	0.0	N_3	10.9	1.1	0.0	N_4	9.1	-9.1	0.0
O	-3.1	-3.2	0.0	O_1	-4.0	3.3	0.0	O_2	3.9	12.8	0.0	O_3	9.4	0.2	0.0	O_4	9.0	-10.4	0.0
P	-3.9	-3.7	0.0	P_1	-3.8	3.6	0.0	P_2	5.8	10.2	0.0	P_3	8.6	-0.5	0.0	P_4	6.8	-8.7	0.0
Q	-5.1	-5.3	0.0	Q_1	-3.3	3.1	0.0	Q_2	6.0	9.5	0.0	Q_3	8.7	-1.1	0.0	Q_4	6.4	-8.9	0.0
R	-6.1	-6.4	0.0	R_1	-1.2	3.8	0.0	R_2	7.0	9.8	0.0	R_3	10.1	-0.8	0.0	R_4	6.8	-6.0	0.0
S	-7.8	-7.4	0.0	S_1	-1.6	4.5	0.0	S_2	6.1	6.8	0.0	S_3	11.3	-1.1	0.0	S_4	6.2	-6.0	0.0
T	-7.6	-5.5	0.0	T_1	-3.1	4.0	0.0	T_2	6.5	6.6	0.0	T_3	11.7	-1.5	0.0	T_4	5.6	-6.6	0.0
U	-7.0	-3.9	0.0	U_1	-4.1	3.8	0.0	U_2	6.8	7.4	0.0	U_3	10.9	-1.7	0.0	U_4	5.4	-5.9	0.0
V	-7.1	-3.8	0.0	V_1	-5.8	3.8	0.0	V_2	8.8	7.9	0.0	V_3	10.5	-2.3	0.0	V_4	5.5	-4.9	0.0
W	-7.9	-4.5	0.0	W_1	-5.4	4.9	0.0	W_2	7.8	5.7	0.0	W_3	11.5	-2.8	0.0	W_4	4.9	-4.5	0.0
X	-9.2	-5.3	0.0	X_1	-8.2	7.6	0.0	X_2	6.8	4.2	0.0	X_3	12.6	-5.3	0.0	X_4	4.5	-5.1	0.0
Y	-10.7	-5.8	0.0	Y_1	-5.4	8.3	0.0	Y_2	7.1	3.9	0.0	Y_3	10.7	-4.5	0.0	Y_4	4.9	-7.6	0.0
Z	-10.1	-4.5	0.0	Z_1	-5.5	9.4	0.0	Z_2	7.0	3.8	0.0	Z_3	8.9	-3.6	0.0	Z_4	4.7	-8.7	0.0

Point	Coordinate (mm)		
	x	y	z
A_5	4.3	-11.0	0.0
B_5	2.9	-7.2	0.0
C_5	2.3	-7.9	0.0
D_5	2.5	-8.5	0.0
E_5	2.3	-11.5	0.0
F_5	1.2	-9.8	0.0
G_5	0.6	-9.9	0.0
H_5	0.8	-11.0	0.0

wideband antenna with 44.6% impedance bandwidth at 10 dB return loss. The proposed antenna achieved a gain of 6 dBi on the average. Likewise, the hybridization of fractals (Koch-Minkowski and Koch-Koch) with Defected Ground Structure (DGS) has been used by authors in [4]. The proposed antenna of dimension 45 × 38.92 × 1.6 mm^3 has an impedance bandwidth of 2.77 GHz (7.74–10 GHz) and 2.46 GHz (7.56–10 GHz); a gain of 5.62 dB and 5.62 dB for Koch-Minkowski and Koch-Koch slots respectively. A slot antenna of the size 0. 35λ × 0.35 λ ×

Figure 2. Typical Papaya leaf.

0. 19λ with a fractional bandwidth of 86% (1.49 GHz–3.75 GHz) at return loss of 10 dB has been proposed in [5].

Furthermore, due to the capability of Bio-inspired structure to achieve reduction in size while improving the perimeter, it has been used in the development of antennas for wideband applications. For instance, bio-inspired structures have been used for a wideband antenna in [11] and [12]. Authors in [11] proposed Maple-leaf Shaped Monopole Antennas with two band rejection techniques for 5.0–6.0 GHz frequency band. The simulated result exhibits impedance bandwidth from 3 to 13 GHz using High Frequency Structure Simulator (HFSS) and CST. The measured impedance bandwidth becomes dual-band (4.1–7.0 GHz) and (8.7–13.3 GHz). The antenna gain range is from 2 - 4.3 dB. Similarly, authors in [12] proposed Jasmine flower-shape based bio-inspired antenna which has 10 Petals at the radius of 10.71 mm of a circular planar monopole and the resonance frequency varied between 8–12 GHz by varying the petal length around 7 mm.

However, none of the authors in the literature considers the use of *Carica Papaya* leaf shape as a bio-inspired structure for antenna applications. Therefore, in this research, a Bio-inspired microstrip Patch Antenna (Bi-MPA) based on perturbation for wideband wireless applications is presented.

2. Antenna design procedure

The design initiator is a circular microstrip patch antenna (CMPA) with radius (R) 13 mm. The initiator was perturbed to realize the bio-inspired (pawpaw leaf) structure presented in Figure 1 (a) and (b) respectively. The proposed structure is built on an epoxy glass (FR4) substrate with a dielectric constant of 4.4, a height of 1.58 mm, a loss tangent of 0.02 and a copper thickness (t) of 18 μm as shown in Figure 1(c) and (e). The size of the substrate is $59.25 \times 35.7 \times 1.58\ mm^3$. The proposed antenna is fed with 50 Ω microstrip feedline and simulated with Ansys® HFSS [13] which is based on the Finite Element Method. The width and length of the feedline are 2.8 mm and 31.2 mm respectively. The ground plane was defected at the two sides, and a rectangular strip was integrated on the defected ground as shown in Figure 1(d). The proposed antenna design parameters specified in Figure 1 are presented in Table 1.

The design equations for circular MPA is given in Eqs. (1) and (2). For resonant frequency (f_r) at 3.06 GHz, the radius of the patch (R) is 13.00 mm using Eqs. (1) and (2).

$$Radius\ (R) = \frac{F}{\sqrt{1 + \frac{2h}{\pi\varepsilon_r F\left\{ln\left(\frac{F\pi}{2h}\right) + 1.7726\right\}}}} \tag{1}$$

and

$$F = \frac{8.791 \times 10^9}{f_r\sqrt{\varepsilon_r}} \tag{2}$$

h is the height of the substrate, ε_r is the dielectric constant of substrate and f_r is the resonant frequency.

The circular patch was designed to determine the radius (the maximum edge) of the proposed Bi-MPA to have resonance at 3.06 GHz as shown in Figure 1(a). Then, the resultant CMPA is perturbed to achieve the proposed Bi-MPA structure. The design data (x-y-z coordinates of each point) of the final structure are presented in Table 2 while Figure 2 shows the picture of a typical *Carica Papaya* leaf shape used in this work except for the slots.

3. Result and discussion

The result of the fundamental structure is presented first in Figure 3 showing the reflection coefficient, the gain, and the radiation pattern. It can be observed that the initiator structure resonated at 2.3 GHz (1.99–3.36 GHz) and 6.4 GHz and 7.91 GHz (5.5–13.1 GHz). It can also be observed that the voltage standing wave ratio of the initiator using Eq. (3) is ≤2 in the operating bands with a maximum gain of 3.13 dB. Nonetheless, communication bands such as WiMAX, WLAN and 5G sub6 GHz bands were band-gapped in the unperturbed circular MPA and these bands are important in wireless communication. Hence, the perturbation of the initiator (CMPA) to realize the bio-inspired microstrip patch antenna (Bi-MPA).

$$VSWR = \frac{1 + S_{11}}{1 - S_{11}} \tag{3}$$

The reflection coefficient (S11) and VSWR of the bio-inspired antenna are presented in Figure 4(a) and (b) respectively. The Bi-MPA shows a wideband characteristic from 1.9 GHz to 6.2 GHz, narrowband at 7.2 GHz (6.99–7.44 GHz) and 9.3 GHz (9.15–9.35 GHz) bands with fractional bandwidth of 106.8%, 6.26% and 2.16% respectively. The proposed antenna resonates at 2.18 GHz, 3.5 GHz, 5.8 GHz, 7.2 GHz and 9.3 GHz with a return loss of -18.5 dB, -14.8 dB, -33.2 dB, -21.5 dB, and -11.3 dB respectively. These resonant frequencies are labelled as f_1, f_2, f_3, f_4, and f_5 respectively. It can be observed from Figure 4(b) that the VSWR ≤2 across the wideband (1.9–6.2 GHz) and the narrow bands. This shows that the proposed antenna is a good candidate for mobile applications as it covers all mobile communication bands except the lower GSM band. The variation between the Bi-MPA and the initiator (CMPA) performance is due to the reduction in the losses and the variation in the surface current density distribution. Perturbation reduces the area covered by the patch and thereby reduces the resultant radius to 9.18 mm from 13 mm while optimizing the perimeter. Using Eqs. (4), (5), (6), (7), and (8), the total conductance due to total loss can be determined by changing radius R (initiator) to R' (Resultant radius of the Bi-MPA structure).

$$Total\ \ conductance\ (GT) = G_R + G_D + G_C \tag{4}$$

$$G_R = \frac{2.39}{4\mu_O h f_r Q_r} \tag{5}$$

$$G_D = \frac{2.39\delta}{4\mu_O h f_r} \tag{6}$$

$$G_C = \frac{2.39\pi(\pi f_r \mu_O)^{-3/2}}{4h^2\sqrt{Q}} \tag{7}$$

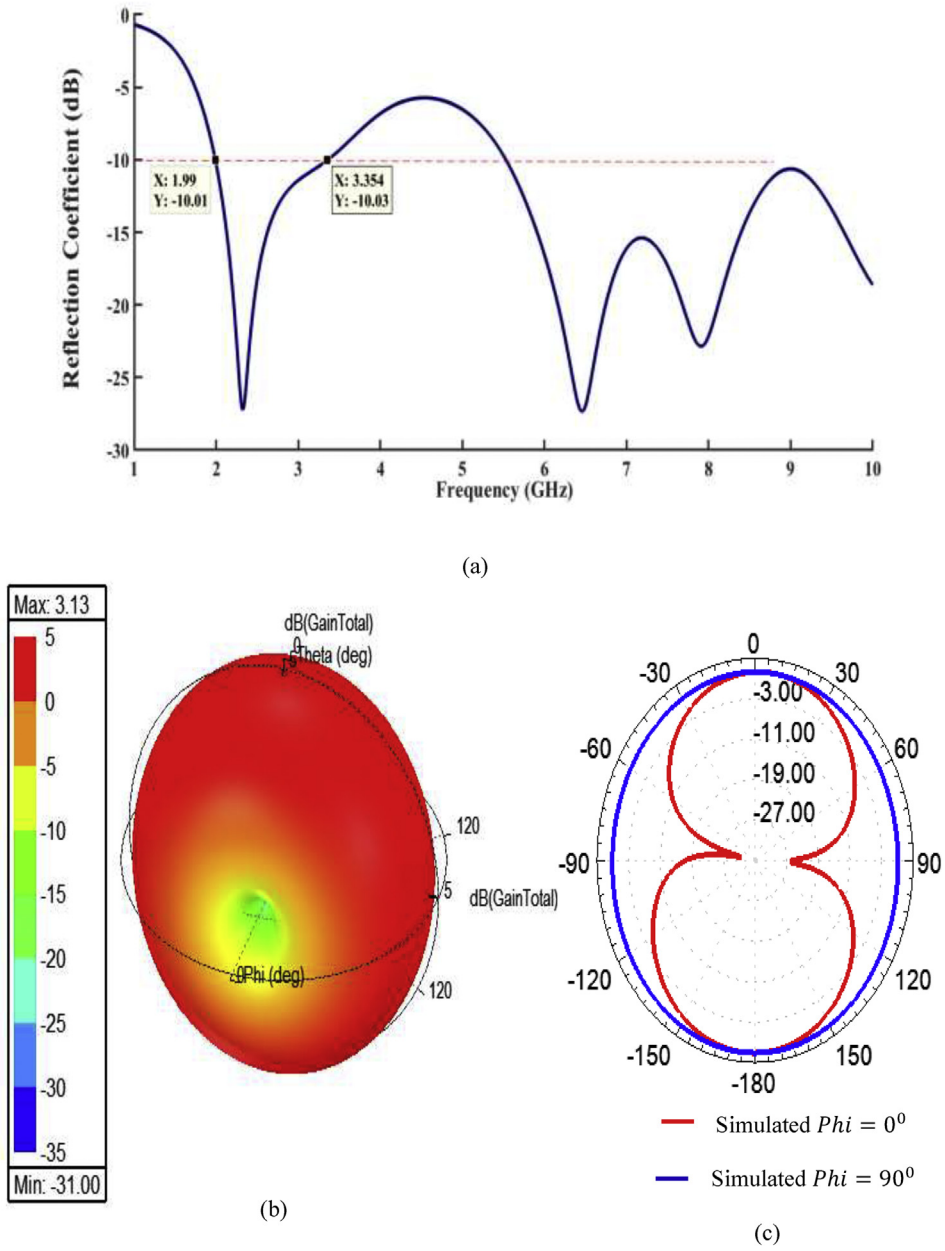

Figure 3. The proposed antenna design initiator (CMPA); (a) Return Loss; (b) Gain; (c) 2D radiation pattern.

$$Q_r = \frac{4R'(\alpha^2 - 1)\varepsilon_r^{3/2}}{h\alpha^3 F \frac{\alpha}{\sqrt{\varepsilon_r}}} \tag{8}$$

Where,

$G_R = Conductance$ due to radiation losses, $G_D = conductance\ due\ to\ dielectric\ losses$ $G_C = Conductance\ due\ to\ homic\ (conduction)\ losses$ $\mu_O = relative\ permeability\ of\ the\ free\ space$, $h = substrate\ height$, $f_r = resonant\ frequency$,

$Q_r = radiation\ coefficient\ and\ Q = Conductivity\ of\ the\ material$

The gain and radiation pattern of the proposed antenna were evaluated across all the useful bands and are presented in Figures 5 and 6 respectively. It can be observed that the gain of the proposed antenna at 1.9 GHz, 2.1 GHz, 2.5 GHz, 3.5 GHz, 4.5 GHz, 5.2 GHz, 5.8 GHz, 7.2 GHz, and 9.3 GHz are 8.41 dB, 8.94 dB, 10.22 dB, 7.72 dB, 4.25 dB, 2.76 dB, 2.74 dB, 4.08 dB, and 2.60 dB respectively. This shows that the proposed antenna demonstrated high gain across the operating frequencies. It can be seen from Figure 6 that the radiation patterns at both the E-plane ($\phi = 0°$) and H-plane ($\phi = 90°$) in all these frequencies are quasi-omnidirectional which show that the proposed antenna is suitable for 2G, 3G, 4G, 5G, WLAN, WiMAX, C-band, and X-band applications.

3.1. Parametric analysis

The parametric study has been done to investigate the effect of the ground plane width, the length, and width of the rectangular strip embedded in the ground plane. Figure 7 shows the effect of Ls (rectangular strip length) on the proposed antenna return loss. It can be observed that five resonant frequencies (f_1, f_2, f_3, f_4, and f_5) are maintained with variation in the return loss value. It can be observed that when Ls is 7.5 mm and 9 mm, the return loss was less than 10 dB at 5.09–5.49 GHz and 5.34–5.64 GHz respectively.

It can be observed from Figure 7 that the fifth resonant frequency (f_5) when Ls is 7.25 mm, 7.5 mm and 7.75 mm has return loss less than 10 dB. This is due to the variation in the surface current distribution which affects the impedance matching at f_3, f_4, and f_5. Whereas impedance

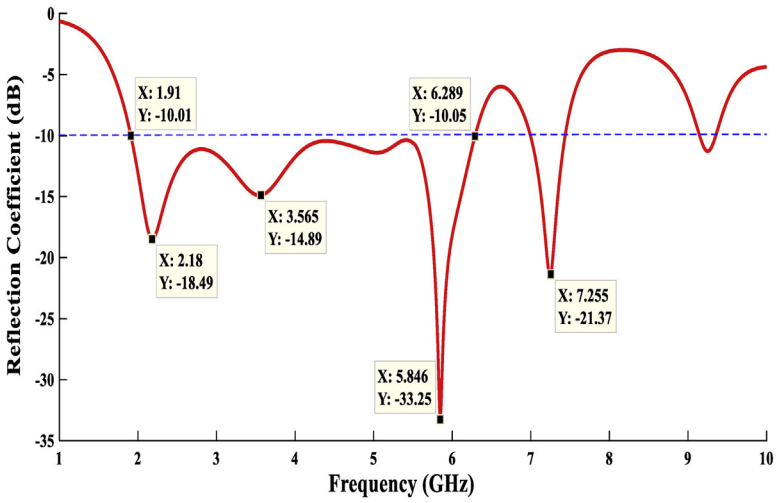

(a)

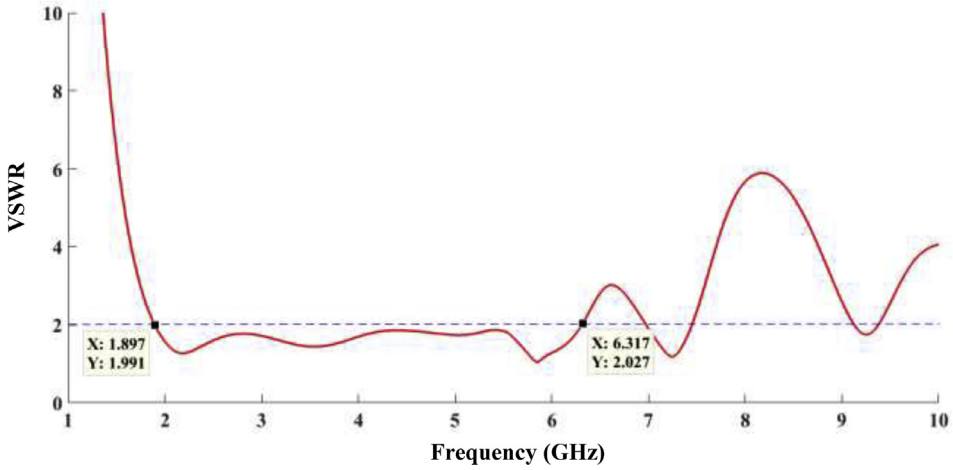

(b)

Figure 4. Proposed Bi-MPA (a) Return loss and (b) VSWR.

matching is enhanced at f_3 and f_4, which in turn improved the return loss at f_3 and f_4, there is a corresponding reduction at f_5.

Figure 8 shows the relationship between RL and W_s. As depicted in the figure, the antenna completely turns to Quadband multiband antenna. It is worthy of note that $W_s = 5.5$ mm shows very good return loss at f_2 (3.3 GHz), f_3 (5.56 GHz) and f_4 (7.38 GHz) which is -44.5 dB, -51.5 dB, and -60 dB respectively while it is flat at f_1 and -14.35 f_2 (9.7 GHz). This shows that the proposed Bi-MPA is a good candidate for multiband applications when W_s is set to be 5.5 mm in the configuration. Figure 9 shows the effect of the ground width on the return loss of the proposed antenna. It was observed that f_1 is completely lost with $W_g = 25$ mm but with a reduction in the 10 dB return loss frequency. $W_g = 30$ mm has better return loss (40 dB) at f_2 compared to 25 mm, 35 mm and 35.7 mm.

Table 3 presents the comparison between the proposed Bi-MPA and the recently published works on wideband antennas. f_l and f_h denote lower and higher frequency respectively. It can be observed that the proposed antenna is compact and has better impedance bandwidth and gain as depicted in Table 3.

4. Conclusion

An extensive study of a Bi-MPA for wideband applications suitable for GSM1900, UMTS, WLAN, LTE, WiMAX, C-band, X-band, and sub6 GHz fifth-generation bands has been presented in this work. It has been shown that the proposed Bi-MPA demonstrated high gain and relatively stable radiation pattern across the entire bands. The significance of this work is the proposal for a wideband antenna that is compact and robust for mobile communication.

Declarations

Author contribution statement

Jeremiah O. Abolade: Conceived and designed the experiments; Performed the experiments; Analyzed and interpreted the data; Contributed reagents, materials, analysis tools or data; Wrote the paper.

Dominic B. O. Konditi: Analyzed and interpreted the data; Contributed reagents, materials, analysis tools or data.

Vasant M. Dharmadhikary: Contributed reagents, materials, analysis tools or data.

Funding statement

This work was sponsored and supported by the African Union through the Pan African University Institute of Basic Sciences, Technology, and Innovation.

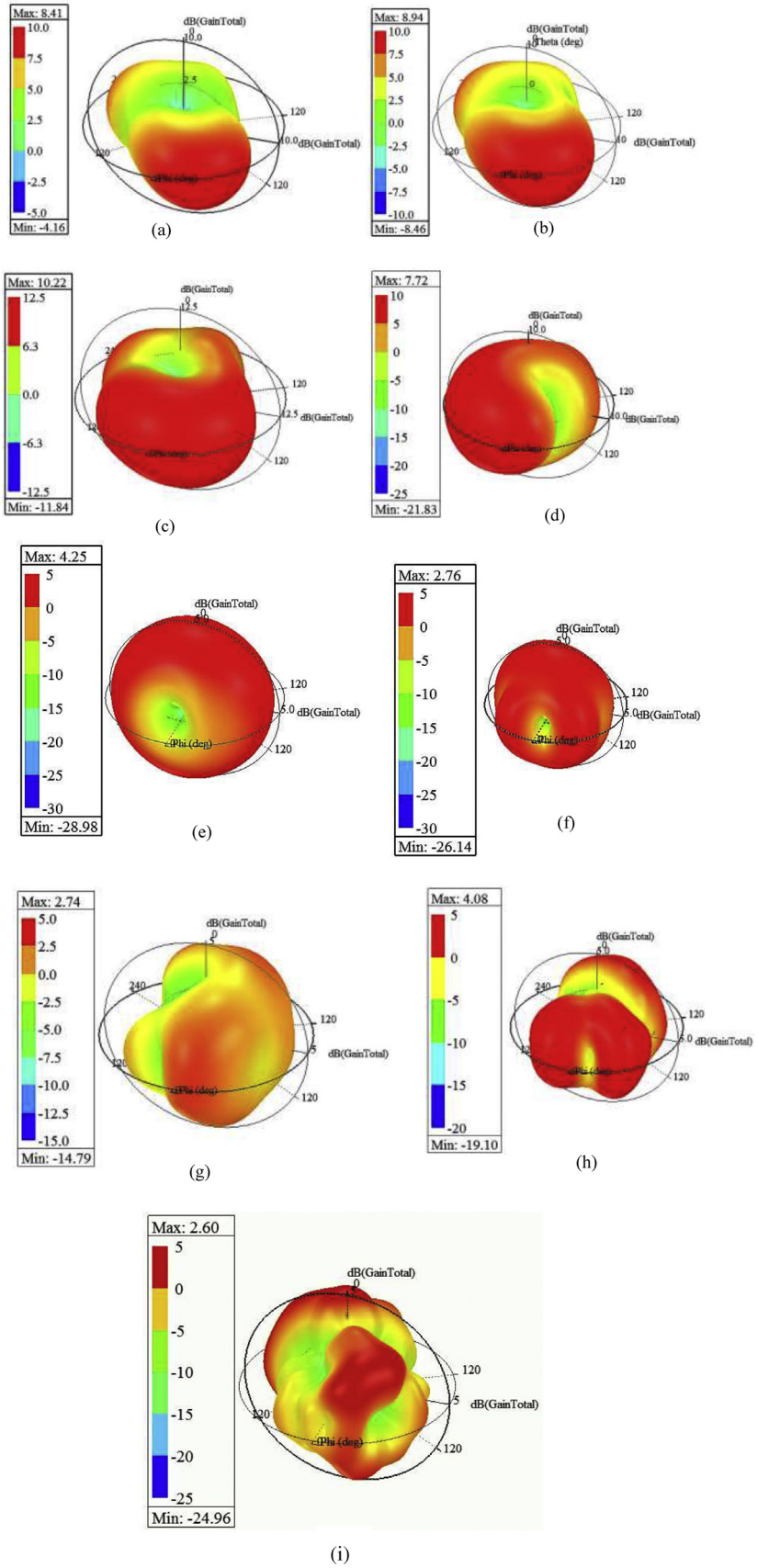

Figure 5. Gain of the proposed antenna at (a) 1.9 GHz, (b) 2.1 GHz, (c) 2.5 GHz, (d) 3.5 GHz, (e) 4.5 GHz, (f) 5.2 GHz; Gain of the proposed antenna at (g) 5.8 GHz, (h) 7.2 GHz, and (i) 9.3 GHz.

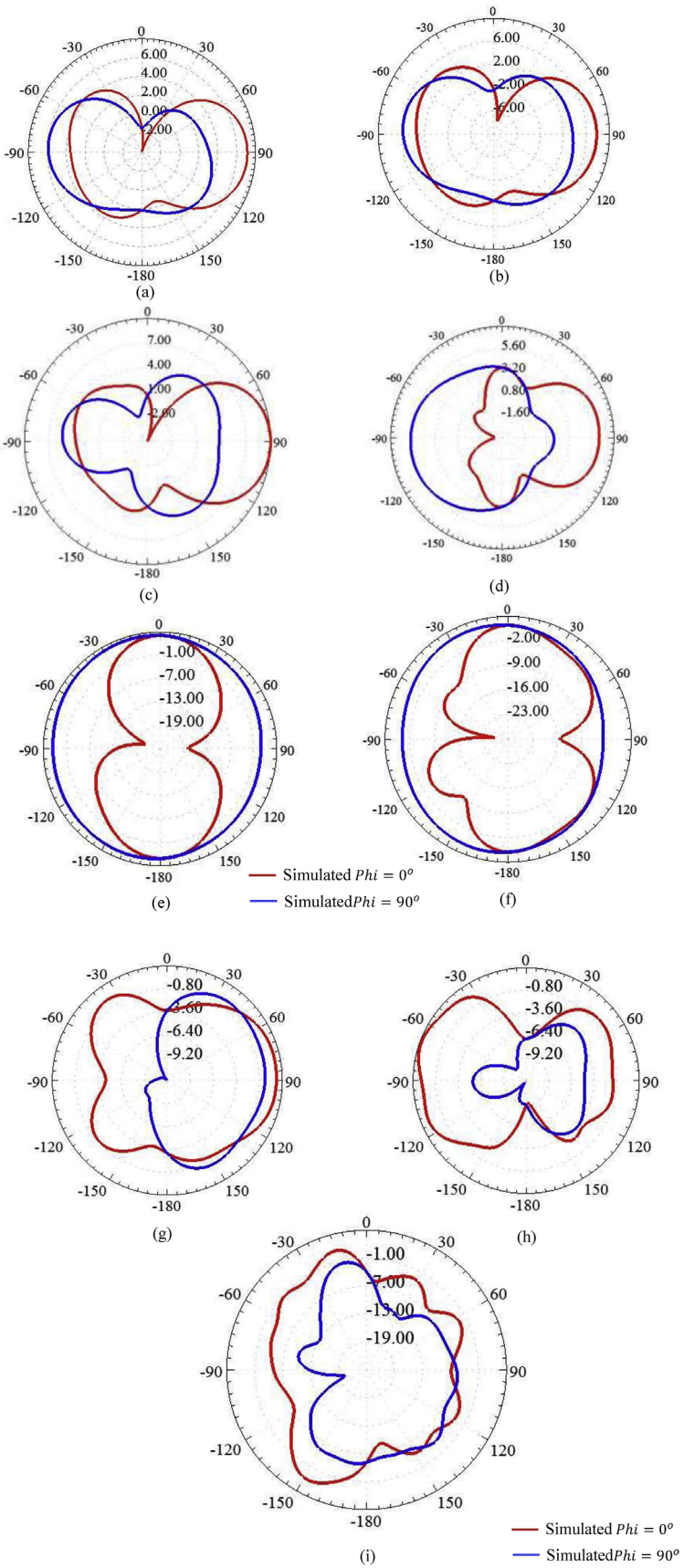

Figure 6. Radiation pattern of the proposed Bi-MPA at (a) 1.9 GHz, (b) 2.1 GHz, (c) 2.5 GHz, (d) 3.5 GHz, (e) 4.5 GHz, and (f) 5.2 GHz; (g) 5.8 GHz, (h) 7.2 GHz, and (i) 9.3 GHz.

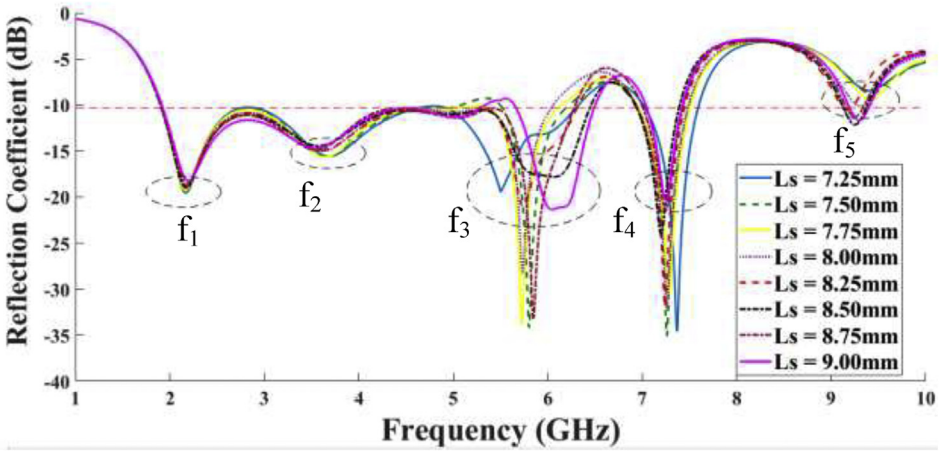

Figure 7. Parametric analysis of the effect of Ls on the return loss of the proposed Bi-MPA antenna.

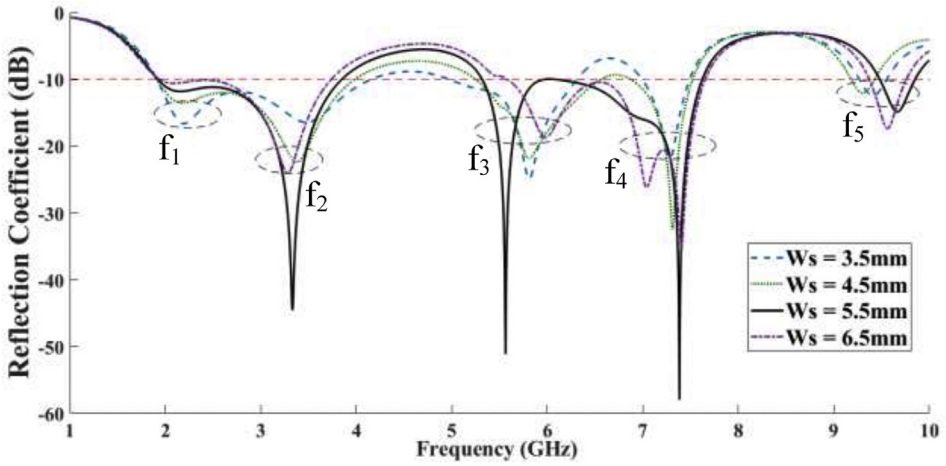

Figure 8. Parametric analysis of the effect of W_s on the return loss of the proposed Bi-MPA antenna.

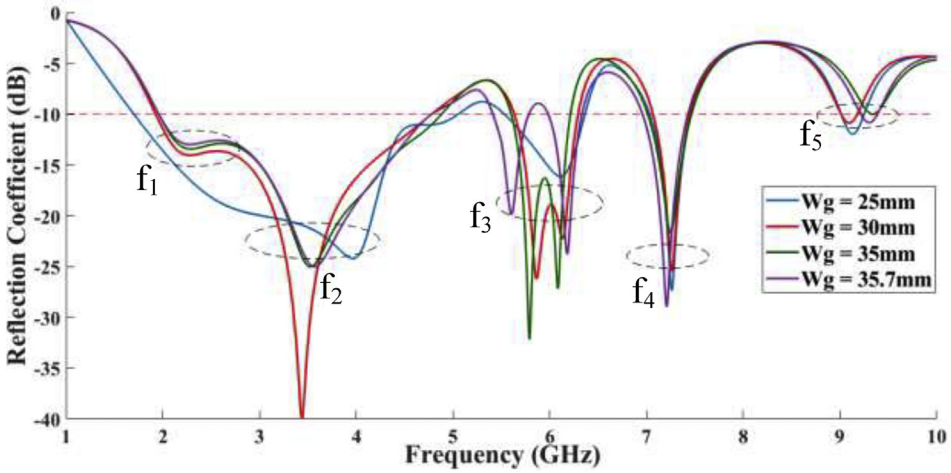

Figure 9. Parametric analysis of the effect of W_g on the return loss of the proposed Bi-MPA antenna.

Table 3. Comparative analysis of Bi-MPA with existing literature.

Reference	Size	f_l/f_h (GHz)	Gain
[5]	$54 \times 54 \times 39$ mm^3	1.49/3.75	7.5 dBic
[2]	$96 \times 64.2 \times 11.5$ mm^3	1.62/2.78	6.1 dBi
[4]	$45 \times 38.92 \times 1.6$ mm^3	7.74/10	5.6 dB
[14]	$40 \times 78 \times 1.6$ mm^3	1.74/2.25	2.58 dB
[11]	$35 \times 35 \times 1.575$ mm^3	3/10.8	2–4.7 dB
[12]	$52.65 \times 35.7 \times 1$ mm^3	3.1/10.6	5.18–5.22 dB
This work (Bi-MPA)	$59.25 \times 35.7 \times 1.58$ mm^3	1.9/6.2	2.6 dB–10.22 dB

Competing interest statement

The authors declare no conflict of interest.

Additional information

No additional information is available for this paper.

References

[1] L. Lu, Y. Jiao, H. Zhang, R. Wang, T. Li, Wideband circularly polarized antenna with stair-shaped dielectric resonator and open-ended slot ground, IEEE Antenn. Wireless Propag. Lett. 15 (2016) 1755–1758.

[2] W. An, X. Wang, H. Fu, J. Ma, X. Huang, B. Feng, Low-profile wideband slot-loaded patch antenna with multiresonant modes, IEEE Antenn. Wireless Propag. Lett. 17 (7) (2018) 1309–1313.

[3] Y. Zhao, E. Wang, D. He, T. Zhang, J. Yang, Design of wideband dual-circularly polarized endfire antenna array on gap waveguide, in: 13th European Conference on Antennas and Propagation, EuCAP 2019, 2019, pp. 1–3.

[4] N. Sharma, V. Sharma, A design of Microstrip Patch Antenna using hybrid fractal slot for wideband applications, Ain Shams Eng. J. 9 (4) (2018) 2491–2497.

[5] Z. Iqbal, S. Lim, Design of a high-gain, wideband, circularly polarized slot antenna, in: 2019 IEEE International Symposium on Antennas and Propagation and USNC-URSI Radio Science Meeting, 2019, pp. 1921–1922.

[6] M. Yang, Y. Sun, F. Li, A compact wideband printed antenna for 4G/5G/WLAN wireless applications, Int. J. Antenn. Propag. 2019 (2019) 1–9.

[7] W. Hu, et al., Compact wideband folded dipole antenna with multi-resonant modes, IEEE Trans. Antenn. Propag. 67 (11) (2019) 6789–6799.

[8] R. Roshan, S. Prajapati, H. Tiwari, G. Govind, A dual wideband monopole antenna for GSM/UMTS/LTE/WiFi/and lower UWB application, in: 2018 3rd International Conference on Microwave and Photonics (ICMAP), 2018, pp. 1–2.

[9] J. Thakur, Compact wideband internal antenna for sub-60 Hz 5G radios, in: 2018 IEEE Indian Conference on Antennas and Propagation (InCAP), 2018, pp. 1–4.

[10] L. Bai, C. Du, Wide-band high-gain DGS antenna system for indoor robot positioning, Int. J. Antenn. Propag. 2019 (2019) 1–10.

[11] O. Haraz, A.-R. Sebak, UWB antennas for wireless applications,, in: Advancement in Microstrip Antennas with Recent Applications, K. Ahmed, Ed. Janeza Trdine 9, 51000 Rijeka, Croatia: intechopen, 2013, pp. 125–152.

[12] A.J.R. Serres, G.K. d-F. Serres, P.F. d-S. Júnior, R.C.S. Freire, J. d-N. Cruz, T.C. De-Albuquerque, A.O. Maciel, P.H. d-F. Silva, Bio-inspired microstrip antenna, in: Trends in Research on Microstrip Antennas, Janeza Trdine 9, 51000 Rijeka, Croatia: Intech, 2017, pp. 87–109.

[13] Ansys Corporation, HFSS electromagnetic suite 19.0, in: Ansoft, Pittsburg (PA), USA, 2019.

[14] F. MRI, H. MI, I. MT, Low specific absorption rate microstrip patch antenna for cellular phone applications, IET Microw., Antennas Propag. 9 (14) (2015) 1540–1546.